City, University of London Institutional Repository

Creep Relaxation in the Presence of Residual Stress

H. Yazdani Nezhad [1] and N. P. O'Dowd
Department of Mechanical, Aeronautical & Biomedical Engineering
Materials & Surface Science Institute
University of Limerick, Limerick, Ireland

Abstract

In this paper, the elastic and elastic-plastic creep behaviour of cracked structures in the presence of a residual stress field have been studied, numerically and analytically. A self-equilibrating residual stress field is introduced by prior mechanical loading. The magnitude of the residual stress field is varied and the corresponding transient crack tip parameter, $C(t)$, is evaluated in single edge notched specimens, using the finite element (FE) method. Since the steady state crack tip parameter, C^*, and redistribution time, t_{red}, are no longer valid for the case of residual stress only (as for this case $C^* \to 0$ and thus $t_{red} \to \infty$), new normalising factors of C_{norm} and t_{norm} are introduced and used to normalise $C(t)$ and time, respectively. Existing analytical solutions are modified based on these normalising factors, and new expressions are developed to describe creep relaxation in the presence of a residual stress field. The values of $C(t)$ obtained from FE analysis are compared to those from the proposed equations. It has been found that the transient $C(t)$ value provides an accurate characterisation of the crack tip fields under residual stress only.

1. Introduction

Manufacturing, joining processing and service load history may result in stress/strain misfits between different regions in a structure. Hence, it is essential to evaluate the influence of residual stress (secondary) field on the creep relaxation behaviour of a structure (see e.g. [1–7]). The influence of combined mechanical and residual stresses has been evaluated in our earlier work [1].

In this paper, the influence of residual stress on creep relaxation behaviour of cracked specimens is studied. The paper studies creep under self-equilibrating residual stress distributions introduced by bending in specimens with a stationary crack under elastic and elastic-plastic conditions. Comparison is provided with existing reference stress solutions. The creep crack tip parameter, $C(t)$, is evaluated under different residual stress levels and material properties using existing formulation and newly developed expressions.

---

[1]Corresponding author: hamed.yazdani-nezhad@ul.ie, Tel: +353 61 202253

2. Theoretical Background

2.1. Definition of Parameters for Creep under Combined Stress

The transient crack tip parameter under creep, $C(t)$, around a stationary crack tip during creep, introduced by mechanical primary loading, is defined as (see e.g. [5])

$$C(t) = \int_{\Gamma \to 0} \dot{W}(\dot{\varepsilon}^c) dy - \mathbf{t} \frac{\partial \dot{\mathbf{u}}}{\partial x} ds, \tag{1}$$

where

$$\dot{W}(\dot{\varepsilon}^c) = \int \boldsymbol{\sigma} d\dot{\varepsilon}^c \tag{2}$$

is the strain energy rate density and $\dot{\varepsilon}^c$ is the creep strain rate. $C(t)$ is a path and time dependent integral, evaluated over paths close to the crack tip ($\Gamma \to 0$).

During the stationary state creep regime, under constant mechanical load, the value of $C(t)$ becomes time and path independent, denoted by C^*,

$$C^* = \int_{\Gamma} \dot{W}(\dot{\varepsilon}^c) dy - \mathbf{t} \frac{\partial \dot{\mathbf{u}}}{\partial x} ds. \tag{3}$$

The value of C^* is independent of a secondary (residual) stress field, as a self-equilibrating stress distributed across the uncracked section of the specimen will relax to zero over long times. The initial J-integral and redistribution time, J_0 and t_{red} respectively, may also be determined by eqs. (4) and (5) respectively with the corresponding primary and secondary stress intensity factors, K^p and K^s respectively (see [1] and [8]),

$$J_0 = \frac{(K^p + K^s)^2}{E'} \tag{4}$$

and

$$t_{red} = \frac{J_0}{C^*}, \tag{5}$$

where $E' = E/\left(1 - \nu^2\right)$ with E and ν as Young's modulus and the Poisson's ratio respectively. Note that eq. (5) is invalid for the case of residual stress only where no mechanical load is applied ($C^* = 0$).

Under conditions where primary creep strains are small, the secondary creep regime is assumed to be the dominant regime [8] and the creep strain is defined by a power law

$$\dot{\varepsilon}^c = \dot{\varepsilon}_0 \left(\frac{\sigma}{\sigma_0}\right)^n = A\sigma^n, \tag{6}$$

where A and n are material constants. The parameters $\dot{\varepsilon}_0$ and σ_0 are normalising strain and stress parameters. In this work, a power law elastic-plastic material response has also been assumed, i.e.

$$\varepsilon^e + \varepsilon^p = \begin{cases} \sigma/E, & \sigma \le \sigma_y \\ \varepsilon_y(\sigma/\sigma_y)^N, & \sigma > \sigma_y \end{cases} \tag{7}$$

where ε^e and ε^p are elastic and plastic (rate independent) strains respectively, σ_y is the yield stress, $\varepsilon_y = \sigma_y/E$ is the yield strain and N is the strain hardening exponent.

For a power law creeping material t_{red} defined via eq. (5) may also be used to provide an estimate of $C(t)$ during the redistribution period (see e.g. [8]),

$$\frac{C(t)}{C^*} = \frac{(1 + t/t_{red})^{n+1}}{(1 + t/t_{red})^{n+1} - \phi}, \tag{8}$$

where, as proposed in [6]

$$\phi = 1 - \frac{C_N C^*}{A J_0}. \tag{9}$$

The constant C_N in eq. (9) depends on the elastic-plastic response of the material. For a power law material response, C_N is given as

$$C_N = \frac{1}{E' \sigma_y^{N-1}}. \tag{10}$$

For the case of residual stress only $C^* \to 0$, and the value of J decreases with time, due to stress relaxation.

The parameter ϕ in eq. (8) depends on the degree of initial plasticity and has the value of unity for elastic-creep behaviour and is zero under widespread plasticity i.e., in the latter case, eq. (8) predicts $C(t) = C^*$ for all time, t.

In R6 [4] the magnitude of the residual stress field is quantified using the dimensionless parameter β,

$$\beta = \frac{K^s}{K^p / L_r}, \tag{11}$$

where L_r denotes the ratio of P/P_L as a measure of the mechanical (primary) load with P as the primary and P_L as the collapse (limit) load. It should be noted that in eq. (11), K^p is a linear function of L_r and therefore β is not dependent on K^p or primary load. In other words, β depends only on the value of K^s, yield stress, $\sqrt{a}$ and the specimen geometry. Thus, eq. (11) is valid for the case of residual stress only. A simplified expression of this equation for single edge notched tension, SEN(T), specimen was derived in [1],

$$\beta = K^s / \left(\sigma_y \sqrt{a} f(a/W) \gamma \left(1 - \frac{a}{W} - 1.232 \left(\frac{a}{W} \right)^2 + \left(\frac{a}{W} \right)^3 \right) \right), \tag{12}$$

where $\gamma = 2/\sqrt{3}$ and $f(a/W)$ is a non-dimensional function of the crack size ratio [3].

2.2. Definition of Parameters for Creep under Secondary Stress Only

Equation (8) cannot be used to obtain $C(t)$ for the case of residual stress only as in this case $C^* = 0$. We therefore examine the general solution. The general solution for $C(t)$ as a function of J may be written as [5, 6]

$$J(t)^{n+1} / C(t) = (n+1) \int_0^t J(t)^n dt + C_A. \tag{13}$$

The constant $C_A = 0$ for an elastic material, and $C_A = C_N J_0^n / A$ under elastic-plastic conditions (see [6] for details). Thus, under elastic conditions:

$$C(t) = \frac{J(t)^{n+1}}{(n+1) \int_0^t J(t)^n dt}, \tag{14}$$

and under elastic-plastic conditions

$$C(t) = \frac{J(t)^{n+1}}{\left((n+1) \int_0^t J(t)^n dt \right) + C_N J_0^n / A} \tag{15}$$

from which eq. (8) has been derived using an approximation for J as a function of time,

$$J(t) = J_0 + C^* t, \tag{16}$$

3

where J_0 may be obtained from eq. (4). Equation (16), found to provide accurate results at short and over long times [5, 6], has been obtained by simply adding the J terms for the short-time solution (the initial J, J_0) to the long-time solution when $dJ/dt = C^*$ [5]. For the case of secondary stress only $C^* = 0$ and $J(t) = J_0$, with J_0 substituted from eq. (4), i.e.

$$J = J_0 = (K^s)^2 / E', \tag{17}$$

where the value of J relates only to the initial residual stress field, K^s, and is not a function of time. Substituting the J expression, $J = J_0$, from eq. (17) into eq. (15) for an elastic-plastic material:

$$C(t) = \frac{J_0^{n+1}}{\left((n+1) \int_0^t J_0^n dt \right) + C_N J_0^n / A} \tag{18}$$

Integrating the denominator,

$$C(t) = \frac{J_0^{n+1}}{(n+1) J_0^n t + C_N J_0^n / A} = \frac{J_0}{(n+1) t + C_N / A}. \tag{19}$$

Under elastic conditions eq. (14) is used, and a similar derivation method from eq. (16) to (19) leads to

$$C(t) = \frac{J_0}{(n+1) t}. \tag{20}$$

A normalising factor is introduced analogous to the reference stress estimation for C^* [8], to present creep relaxation curves (normalised $C(t)$ values),

$$C_{norm} = \sigma_{ref}^0 \dot{\varepsilon}_{ref}^0 R \tag{21}$$

where σ_{ref}^0 and $\dot{\varepsilon}_{ref}^0$ are an initial reference stress and strain rate, respectively, and R is a crack size dependent factor for secondary stress [8],

$$R = \left(\frac{K^s}{\sigma_{ref}^0} \right)^2. \tag{22}$$

Using the power law relation, eq. (6) for $\dot{\varepsilon}_{ref}^0$ in eq. (21), a normalising value of $C(t)$ is then defined as

$$C_{norm} = A \left(\sigma_{ref}^0 \right)^{n-1} (K^s)^2. \tag{23}$$

In this work for an equilibrating residual stress field, σ_{ref}^0 is taken as an estimation of initial reference stress near the crack tip, and is defined as [3]

$$\sigma_{ref}^0 = \sigma_{ref}^p \left(\frac{K^p + K^s}{K^p} \right) = \sigma_{ref}^p + K^s \left(\frac{\sigma_{ref}^p}{K^p} \right), \tag{24}$$

where σ_{ref}^p is the reference stress due to the primary stress.

In eq. (24), $\sigma_{ref}^p = 0$ and σ_{ref}^p / K^p is a geometry dependent factor [1]. Thus, eq. (24) is simplified to

$$\sigma_{ref}^0 = \left(\frac{K^s}{\sqrt{a}} \right) \left(\frac{1}{f(a/W) h(a/W) \gamma} \right), \tag{25}$$

where (see section 2.1)

$$h(a/W) = 1 - \frac{a}{W} - 1.232 \left(\frac{a}{W} \right)^2 + \left(\frac{a}{W} \right)^3. \tag{26}$$

4

A linear relation between σ_{ref}^0 and β can be made for creep under residual stress only. From eq. (11)

$$\frac{\beta}{K^s} = \frac{L_r}{K^p}. \tag{27}$$

Using eq. (24), σ_{ref}^0 can be written as

$$\sigma_{ref}^0 = K^s \left(\frac{\sigma_{ref}^p}{K^p} \right) = K^s \left(\frac{\sigma_y L_r}{K^p} \right), \tag{28}$$

where $\sigma_{ref}^p = \sigma_y L_r$ [8]. L_r/K^p is substituted from eq. (27) in eq. (28),

$$\sigma_{ref}^0 = \beta \sigma_y. \tag{29}$$

Equation (29) demonstrates a linear relation between σ_{ref}^0 and β, and is equivalent to eq. (25).

Note that in [3], eq. (24) is used only for an elastic-creep material. Here, it is also used for an elastic-plastic creep material. An alternative approach for the evaluation of σ_{ref}^0 for an elastic-plastic creep material has been proposed in [9], and used in [1] for creep under combined stress. Our investigations showed that the alternative approach and eq. (24) provide an almost identical value for σ_{ref}^0 for the case of residual stress only.

A normalising time is also needed in this work. Note that eq. (5) can not be used to define an appropriate t_{red} for creep under residual stress only. Thus, C^* is replaced by C_{norm} in eq. (5), and a normalizing time, t_{norm}, is provided by

$$t_{norm} = \frac{J_0}{C_{norm}}. \tag{30}$$

Equation (19) can then be normalised using C_{norm} and t_{norm} and rewritten as

$$\frac{C(t)}{C_{norm}} = \frac{1}{(n+1)t/t_{norm} + \phi'}. \tag{31}$$

In eq. (31)

$$\phi' = \frac{C_N C_{norm}}{A J_0}. \tag{32}$$

Under elastic-creep conditions $\phi' = 0$ in eq. (31). It may be noted that eq. (31) under elastic-creep conditions has the same form as the equation developed for primary loading by Riedel [10], under elastic conditions at short times, with C^* replaced by C_{norm}. The accuracy of eq. (31) in the prediction of creep relaxation in the presence of residual stress is examined in sections 4.3 and 4.4.

2.3. $C(t)$ approximations using the reference stress

An alternative approach to the evaluation of $C(t)$, based on the reference stress approach has been proposed in [7], for the general case of combined primary and secondary stress, as

$$\frac{C(t)}{C_{norm}} = \frac{\left(\sigma_{ref}(t)/\sigma_{ref}^p \right)^{n+1} \left(\varepsilon_{ref}(t)/\varepsilon_{ref}^0 \right)^{n+1}}{\Psi(t) \left(\left(\varepsilon_{ref}(t)/\varepsilon_{ref}^0 \right)^{n+1} - 1 \right) + \left(1 - \sigma_{ref}^0/E'\varepsilon_{ref}^0 \right)}, \tag{33}$$

where σ_{ref} is the total reference stress, ε_{ref} and ε_{ref}^0 are the total and initial reference strains, respectively, and σ_{ref}^p is the reference stress due to the primary stress. In our equation, C^* which is the normalising value in [7] is replaced by C_{norm} for the case of residual stress only. The total reference

5

stress, σ_{ref}, is time dependent and its relaxation from the initial value, σ_{ref}^0, can be evaluated by integration [3]

$$\dot{\sigma}_{ref} = -\frac{E'}{Z}\left(\dot{\varepsilon}_{ref} - \dot{\varepsilon}_{ref}^p\right), \tag{34}$$

where $\dot{\varepsilon}_{ref}$ and $\dot{\varepsilon}_{ref}^p$ are the creep strain rates due to total and primary reference stresses respectively, and $Z \geq 1$ is the elastic follow-up factor. Using eq. (6) $\dot{\varepsilon}_{ref}^p = 0$ as $\sigma_{ref}^p = 0$. Equation (34) is then further simplified to

$$\dot{\sigma}_{ref} = -\frac{E'}{Z}\dot{\varepsilon}_{ref} = -\frac{AE'}{Z}\sigma_{ref}^n. \tag{35}$$

A very low relaxation rate of σ_{ref} is obtained from this equation for the case of residual stress only i.e. σ_{ref} slightly decreases with time from its initial value, σ_{ref}^0.

Equation (34) has been solved in this work using a code written in MATLAB [11] with the initial condition $\sigma_{ref} = \sigma_{ref}^0$ at $t = 0$. Consequently, ε_{ref} may be obtained by

$$\varepsilon_{ref} = \varepsilon_{ref}^0 + \varepsilon_{ref}^c = \varepsilon_{ref}^0 + A\int \sigma_{ref}^n dt, \tag{36}$$

with the initial condition $\varepsilon_{ref} = \varepsilon_{ref}^0$ at $t = 0$. ε_{ref}^0 is calculated from the strain-stress relationship of the material, i.e. eq. (7) with σ replaced by σ_{ref}^0.

To evaluate Z in eq. (34), following [7], [9] and [12], the evolution of J as a function of time, obtained from FE solutions, is matched to the equation below when primary stress is zero, with Z as the only unknown in the equation

$$\frac{J(t)}{J_0} = \left(\frac{\sigma_{ref}(t)}{\sigma_{ref}^0}\right)\left(1 + \frac{\dot{\varepsilon}_{ref}^p}{\varepsilon_{ref}^0}t - (Z-1)\frac{\sigma_{ref}(t) - \sigma_{ref}^0}{E'\varepsilon_{ref}^0}\right), \tag{37}$$

which can be simplified, as $\dot{\varepsilon}_{ref}^p = 0$, to

$$\frac{J(t)}{J_0} = \left(\frac{\sigma_{ref}(t)}{\sigma_{ref}^0}\right)\left(1 - (Z-1)\frac{\sigma_{ref}(t) - \sigma_{ref}^0}{E'\varepsilon_{ref}^0}\right). \tag{38}$$

For the case of residual stress only, the parameter $\Psi(t)$ in eq. (33) is defined by

$$\Psi(t) = \frac{Z}{\left(\sigma_{ref}^p/\sigma_{ref}(t)\right)^n + (Z-1)}, \tag{39}$$

which can be simplified to

$$\Psi(t) = \frac{Z}{Z-1}, \tag{40}$$

for the case of residual stress only.

The accuracy of eqs. (31) and (33) for the prediction of $C(t)$ under secondary stress only will be examined in section 4.

3. Computational Approach

The modelling framework is described schematically in Fig. 1: a stress distribution is first introduced by elastic-plastic bending of the uncracked specimen (step 1). Unloading of the specimen introduces a residual (secondary) stress distribution (step 2). In this work, both elastic-plastic creep and elastic-creep analyses have been carried out. In the latter case, the elastic-plastic residual stress distribution

obtained in step 2, is introduced as an initial stress to an elastic specimen in step 3 (before introducing the crack), using the initial stress allocation method in ABAQUS [13]. The residual stress field taken from the elastic-plastic model needs to be equilibrated consistently with the elastic material in the new model. Following the approach in [14], a linear iterative equilibrating procedure is used to obtain the desired residual stresses in the elastic specimen (initially stress-free).

In step 3, a sharp crack is introduced to the body by releasing the nodal constraints up to a distance a, where a is the crack length. Crack face nodes were released simultaneously using small time increments. Residual stress redistribution is then allowed to occur due to creep.

The level of residual stress is varied by loading the uncracked specimen up to $L_r = 1.0$ ($P = P_L$), 2.0 ($P = 2P_L$) and 3.0 ($P = 3P_L$) and a subsequent unloading. Corresponding β values at different material response are tabulated in table 1.

3.1. Finite Element Model

The FE mesh used in the analysis is illustrated in Fig. 2, which has also been used in previous work [1]. Concentric elements provide an accurate extraction of crack tip parameters, with five rings of elements adjacent to the crack tip (shaded elements), from which an average value of the creep characterising parameter is extracted (Fig. 2b), excluding the first ring. Two dimensional 4-node quadratic elements discretise the model. Linear 'hybrid' plane strain (CPE4H in ABAQUS [13]) and plane stress (CPS4) elements have been used. Half of the specimen has been modelled to reduce the number of calculations. The mesh consists of 2415 elements and 2552 nodes for each model. The focused mesh consists of 46 rings spanning a radial distance $0 < r/a < 0.9$ with r the radial distance from the crack tip. Each ring consists of 30 elements spanning the crack tip. Internal element rings from which $C(t)$ values are extracted typically span a radial distance $0 < r/a < 3\times10^{-4}$ (Fig. 2b). The mesh sensitivity of the characterising parameters was examined to determine the appropriate crack tip element size (discussed in detail in [1]). It was shown that with increasing mesh resolution, the evolution of $C(t)$ converges to a single distribution. The suitable element size (d) adjacent to the crack tip was found to be $d/a = 3 \times 10^{-5}$.

Equations (6) and (7), are used with power law creep and strain hardening exponents, n and N (= 3 and 10). In the case of an elastic-plastic creep material, the case of $N = n$ is examined. Isotropic strain hardening is assumed.

4. Results

4.1. Residual Stress Distributions

Three typical residual stress profiles, characterised by β or K^s, along the crack direction introduced by different levels of mechanical loads are examined (see table 1) with the crack to be inserted in the region $0 < x/W < 0.2$ where the residual stress is positive (see Fig. 3). As in [1], the crack sizes are $a/W = 0.07$ and 0.15 in this work which are consistent with these values.

When transferring the residual stress distribution from the elastic-plastic analysis to the elastic creep analysis, stresses are extracted from the elastic-plastic model in the region $0 < y < W/5$, with W the width of specimen (see Fig. 2a) and introduced to the identical element set along the crack path in the elastic model (steps 2 and 3 in Fig. 1a).

4.2. Evaluation of J-integral

The value of J_0 has been obtained from the FE analysis using the modified J expression, introduced in [14, 15], which provides a path independent J value in the presence of residual stress.

Figure 4 compares the residual J values from ABAQUS and the modified J expression [15] at three residual stress levels ($\beta = 0.13$, 0.33 and 0.41, see table 1). It is seen in Fig. 4 that the value of J from ABAQUS shows significant path dependence while the value obtained using the method in [15] is positive and path independent over 30 contours. It may also be noted that J_0 obtained from the FE analysis is consistent with the small scale yielding relationship, eq. (4), where K^s is evaluated using a Green's function approach and $K^p = 0$ (see also [15]).

4.3. Elastic-Creep Analysis

4.3.1. Estimate of $C(t)$ based on J_0

Figure 5 shows the FE results under elastic-creep conditions for two creep exponents and two a/W ratios. The solid line represents the analytical result from eq. (31). Note that eq. (31) is independent of crack geometry though the FE analysis predicts some dependence on a/W.

As seen in Fig. 5 for $n = 3$, eq. (31) overestimates the value of $C(t)$ compared to the FE solution and thus provides conservative predictions. For $n = 10$ and $a/W = 0.15$ good agreement is obtained for $t/t_{norm} > 0.1$. For $n = 10$ and $a/W = 0.07$ slightly non-conservative predictions are obtained for $\beta = 0.18$ and 0.45 but the overall agreement with the FE prediction is good. It is also seen that the normalising factors, t_{norm} and C_{norm}, provide a near unique interpretation for the $C(t)$ results i.e. the result is weakly dependent on the amplitude of the residual stress field, β.

Figure 6 compares the FE prediction of the evolution of J for $n = 3$ and $n = 10$. Though J is almost constant with time for $t/t_{norm} > 20$, for $n = 10$ it significantly deviates from J_0 initially. This may explain the overestimation of $C(t)$ at short times for $n = 3$.

4.3.2. Estimate of $C(t)$ based on reference stress method

Figure 7 shows the dependency of $J(t)/J_0$ on Z values for two values of β. As seen, the most suitable value of Z for this case ($n = 3$, secondary stress only, SENB) is 1.01. Figure 8 compares the numerical and analytical $C(t)$ solutions from eqs. (31) and (33). Here attention is focused on the region $C(t)/C_{norm} < 1$ to allow clear comparison of the estimation procedures (compare Fig. 5).

Figure 8(a) shows that the results from eq. (31) are conservative and in reasonable agreement with the FE results. However, eq. (33), the full reference stress solution shows a rapid relaxation for $t/t_{norm} << 1$ providing a non-conservative prediction. Figure 8(b) shows that for $n = 10$, eq. (33) again provides a non-conservative prediction. The results from eq. (31) are conservative, except slightly non-conservative for $\beta = 0.18$, and in good agreement with the FE results.

4.4. Elastic-Plastic Creep Analysis

Figure 9 presents the evolution of $C(t)$ values under elastic-plastic creep conditions. Under elastic-creep conditions a near unique representation of the $C(t)$ values has been obtained from the FE analysis (see Fig. 5). Thus a representative elastic result is presented for the case of elastic-plastic in Fig. 9 (shaded symbols). As seen in the figure, the effect of plasticity is to reduce $C(t)$, relative to this elastic-creep solution, with the effect increasing with an increase in secondary stress, as quantified by β. (Note that the value of C_{norm} is not the same for each value of β). For $N = n = 3$, Fig. 9(a), the normalised $C(t)$ reduces rapidly to zero for $\beta > 0.3$, a trend not observed for $N = n = 10$, Fig. 9(b).

The solid and dash lines in Fig. 9 illustrate the elastic-plastic predictions, eq. (31). Equation (33) provides a non-conservative prediction in all cases, and is not shown. In Fig. 9(a), when $\phi' > 0.1$, eq. (31) predicts that $C(t) \simeq 0$ for all values of t. It may be seen that for $n = 3$, very good agreement is obtained between the FE solution and eq. (31).

For $n = 10$, Fig. 9(b), the estimate from eq. (31) is in very good agreement with the FE results for all β values. For $\beta = 0.18$ and 0.45, $\phi' < 0.01$, eq. (31) provides results close to the result of elastic-creep expression. Slightly non-conservative results is provided when $\beta = 0.18$.

The results in Fig. 9 may be interpreted physically in terms of typical conditions for a component operating at high temperature. The FE analysis predicts that for $n = 10$ the value of $C(t)$, and hence crack tip stresses and creep strain rates, will be negligible for $t > t_{norm}$. From section 2.2, taking typical values, $A = 5.813 \times 10^{-30}$ (stress in MPa, time in hr.) [8], $E' = 200$ GPa, $a = 1$ cm, $K^s = 20$ MPa$\sqrt{\mathrm{m}}$, we find $t_{norm} \approx 1700$ hrs.

5. Conclusion

Creep relaxation in the presence of residual stress only was examined. It was found that the effect of plasticity is to reduce the magnitude of $C(t)$ compared to an elastic-creep material.

These investigations led to the definition of a normalising factor C_{norm} and a normalising time, t_{norm}. It was found that the simple estimation scheme proposed, eq. (31), provides a conservative result in good agreement with the FE solution. Equation (33) based on the existing reference stress method, generally provides a non-conservative prediction. As was seen for creep under the combined stress in [1], it is evident here that care must be taken in the use of the $C(t)$ estimation schemes in structural analysis, with any non-conservatism in these estimates accounted for elsewhere within the procedure.

References

[1] H. Yazdani Nezhad and N.P. O'Dowd. Study of creep relaxation under combined mechanical and residual stresses. *J. Engng. Fract. Mech.*, 93:132–152, 2012.

[2] N.P. O'Dowd, K.M. Nikbin, R.C. Wimpory, F.R. Biglari, and M.P. ODonnell. Computational and experimental studies of high temperature crack initiation in the presence of residual stress. *Pressure Vessel Technology*, 130, 2008.

[3] *R5:An Assessment Procedure for the High Temperature Response of Structures*. Revision 3, British Energy Generation Ltd.,Gloucester,UK. 2003.

[4] *R6:Assessment of the Integrity of Structures Containing Defects*. Revision 4, British Energy Generation Ltd.,Gloucester,UK. 2009-10.

[5] R.A. Ainsworth and P.J. Budden. Crack tip fields under non-steady creep conditions -1. estimates of the amplitude of the fields. *J. Fat. Fract. Engng. Mater. Struct.*, 13(3):263–276, 1990.

[6] J. Joch and R.A. Ainsworth. The effect of geometry on the development of creep singular fields for defects under step-load controlled loading. *J. Fat. Fract. Engng. Mater. Struct.*, 15(3):229–240, 1992.

[7] R.A. Ainsworth, D.W. Dean, and P.J. Budden. *Creep and Creep-fatigue Crack Growth for Combined Loading: Extension of the advice in R5 Volume 4/5 Appendix A3*. British Energy Report E/REP/BDBB/0059/GEN/04, 2005.

[8] G.A. Webster and R.A. Ainsworth. *High Temperature Component Life Assessment*. 1994.

[9] Y. Lei and D.W. Dean. Finite element validation of the method used to estimate the creep crack tip charactering parameters for combined primary and secondary stresses. In *Proceeding of 19th conference on Structural Mechanics in Reactor Technology (SMiRT19)*, 2007.

[10] H. Riedel. *Fracture at High Temperatures*. 1987.

[11] *MATLAB v7.1. User's Manual.*

[12] R.A. Ainsworth. The treatment of combined primary and secondary stresses in elastic-plastic and creep fracture. In *Proceeding of the European Conference on Fracture (ECF18)*, 2010.

[13] *ABAQUS v6.9. User's Manual.*

[14] Y. Lei, N.P. O'Dowd, and G.A. Webster. Analysis of a crack in a residual stress field. *Int. J. Fract.*, 106(3):195–216, 2000.

[15] Y. Lei. J-integral evaluation for cases involving non-proportionalstressing. *J. Engng. Fract. Mech.*, 72(4):577–596, 2005.

6. Tables

Table 1: variation of β at different loading level for $a/W = 0.07$

| L_r	$n = 3$	$n = 10$
1.0	0.13	0.18
2.0	0.33	0.45
3.0	0.41	0.50

(a)

(b)
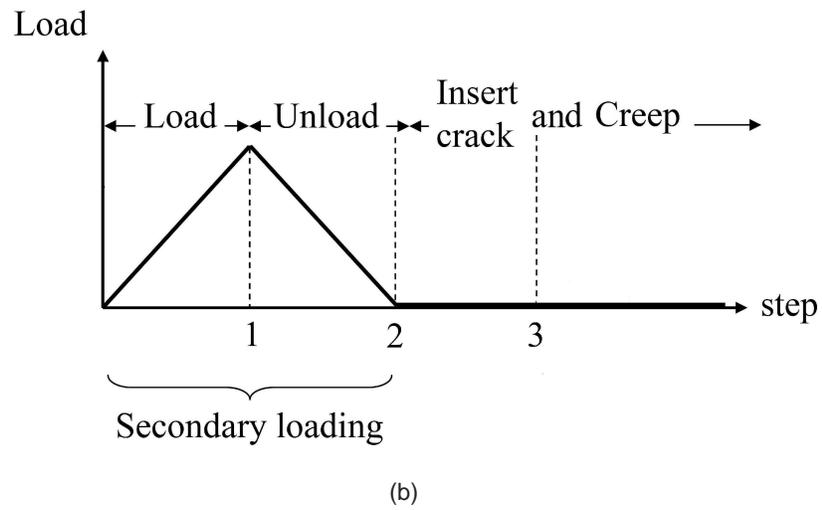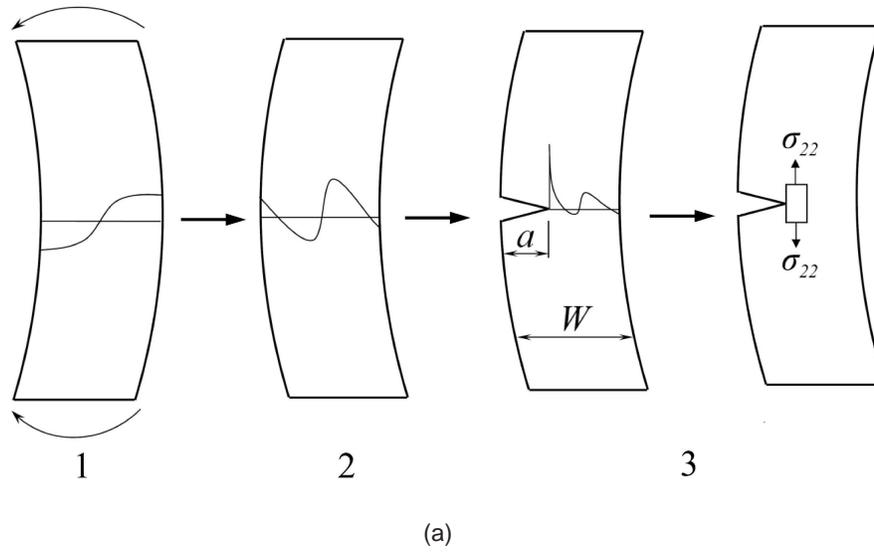
Figure 1: Combined loading strategy for elastic-plastic analysis; (a) schematic loaded model, (b) loading steps including primary and secondary loads
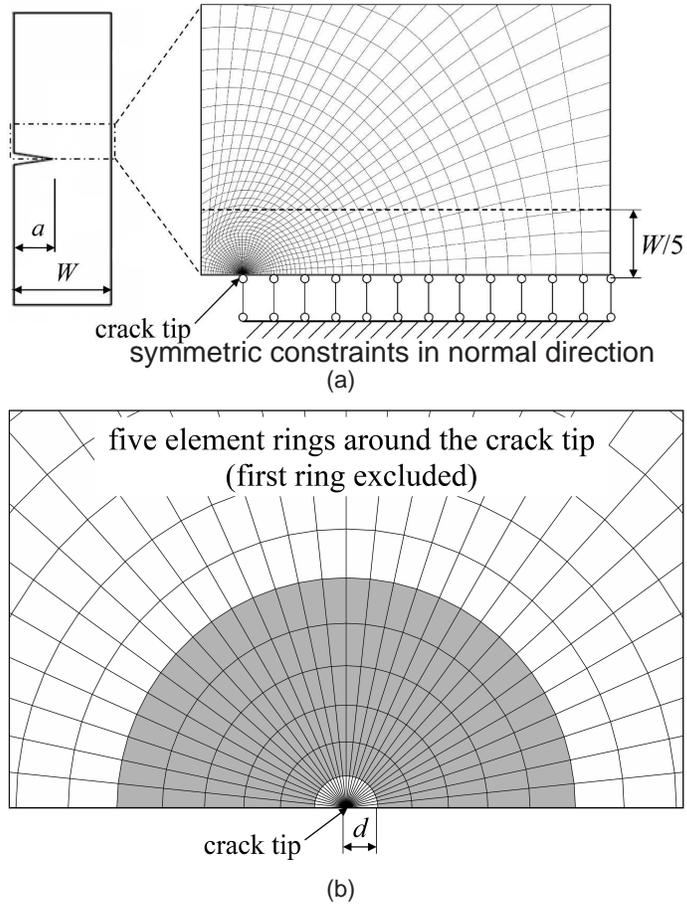
Figure 2: FE model; (a) typical mesh used in analysis (element rows in the region of $W/5$ are selected to extract and introduce the stress values), (b) five rings of elements adjacent to the crack tip (shaded elements) to extract creep characterising parameters (first ring excluded). here d is the size of the crack tip element.
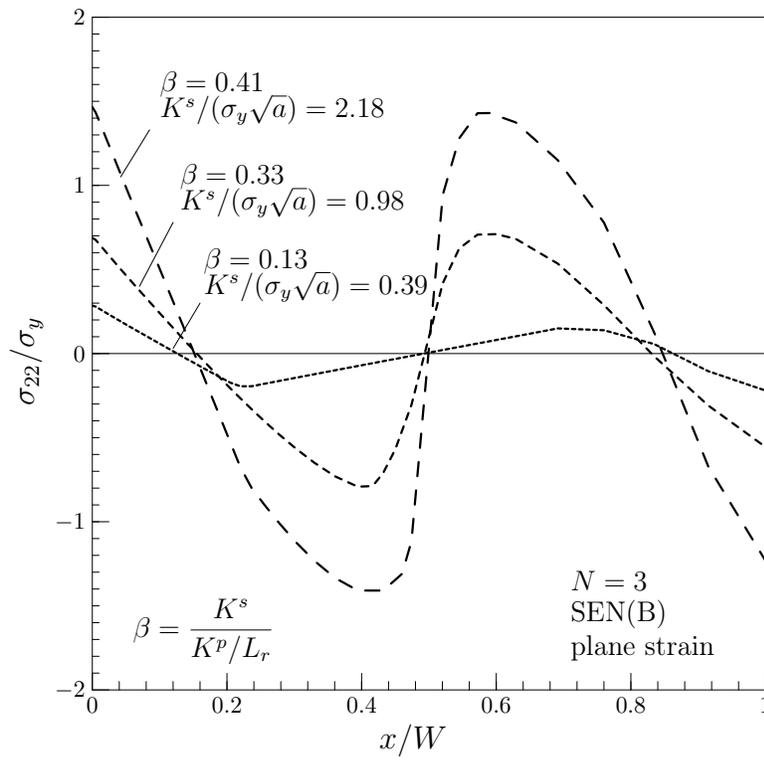
Figure 3: Residual stress (σ_{22}) distribution for SEN(B) and $N = 3$ after unloading the specimen (step 2 in Fig. 1)
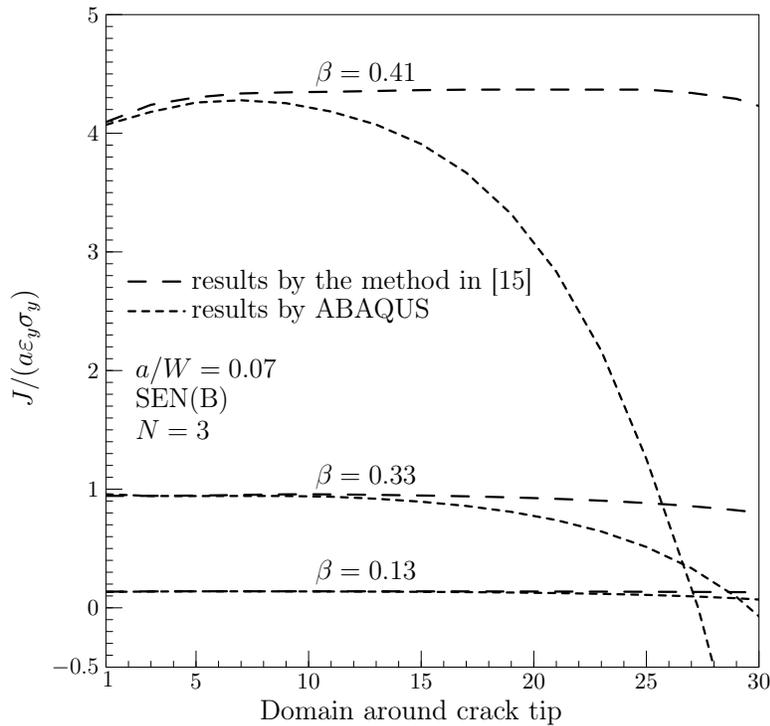
Figure 4: Comparison of residual J values from the expression in [15] and ABAQUS for $\beta = 0.13$, 0.33 and 0.41.

14
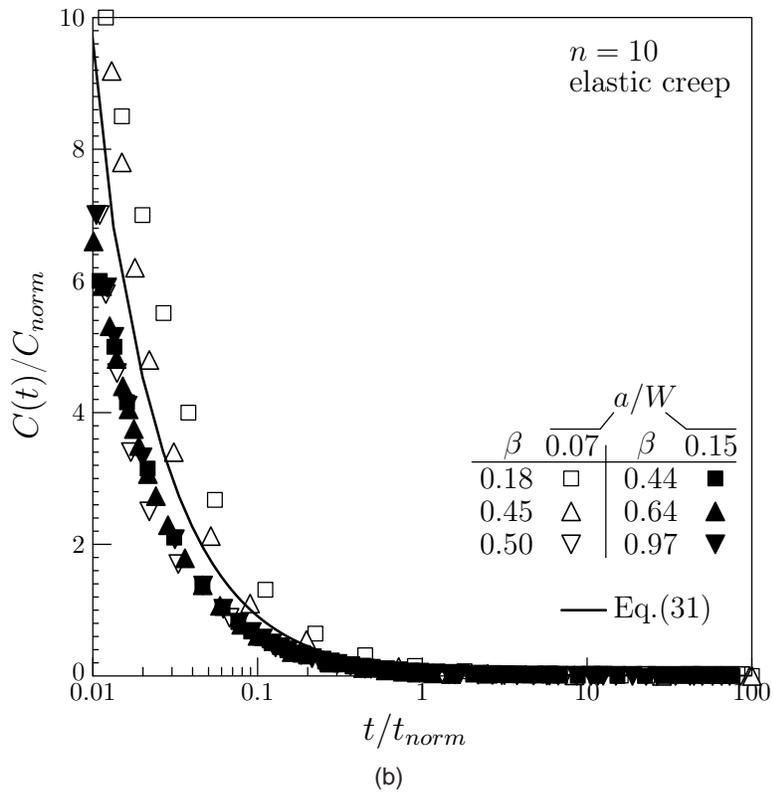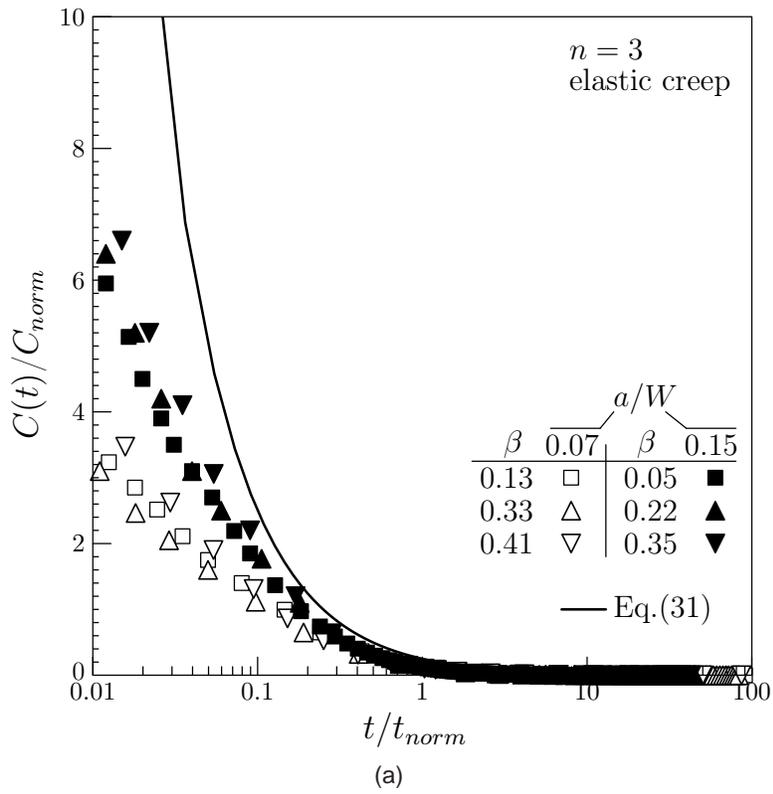
Figure 5: Comparison of evolution of $C(t)$ for elastic-creep conditions under residual stress only at different β values for $a/W = 0.07$ and $a/W = 0.15$ for; (a) $n = 3$, (b) $n = 10$

15
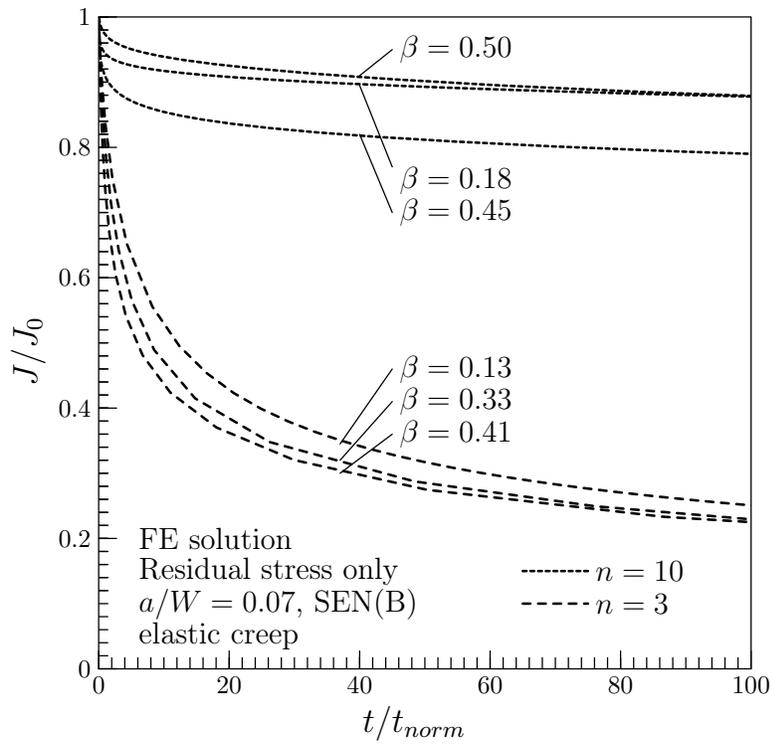
Figure 6: Comparison of evolution of $J(t)$ for elastic-creep conditions under residual stress only at different n values for $a/W = 0.07$
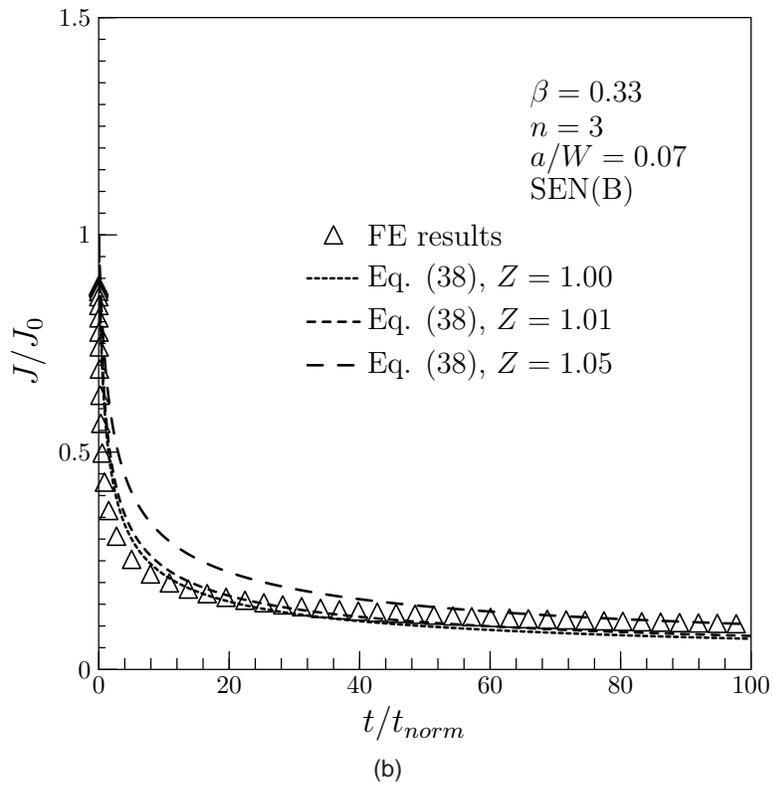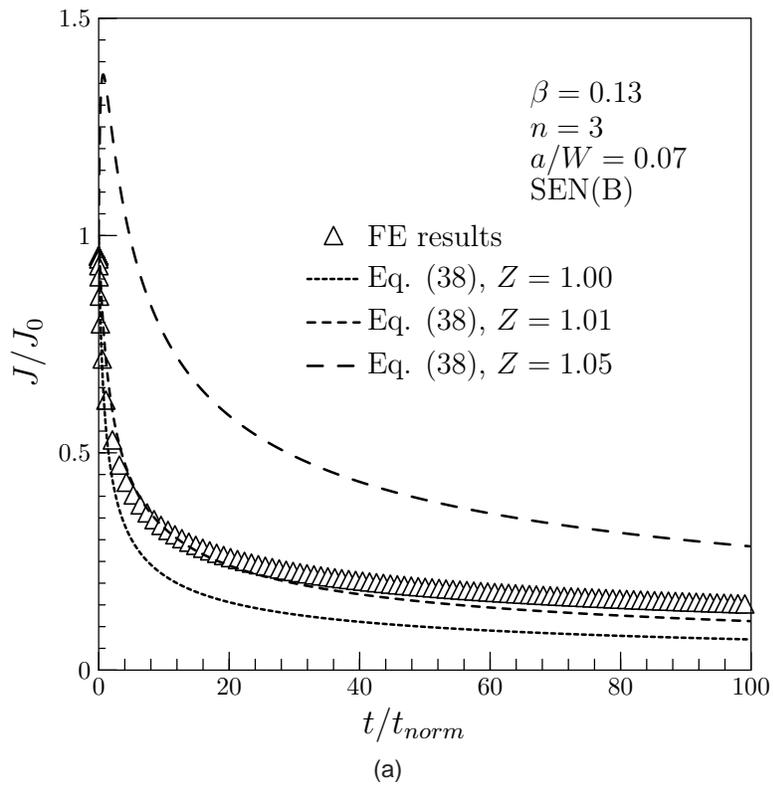
Figure 7: Comparison of predicted normalised J values with the FE results under secondary stress only for $a/W = 0.07$ and $n = 3$; (a) $\beta = 0.13$, (b) $\beta = 0.33$
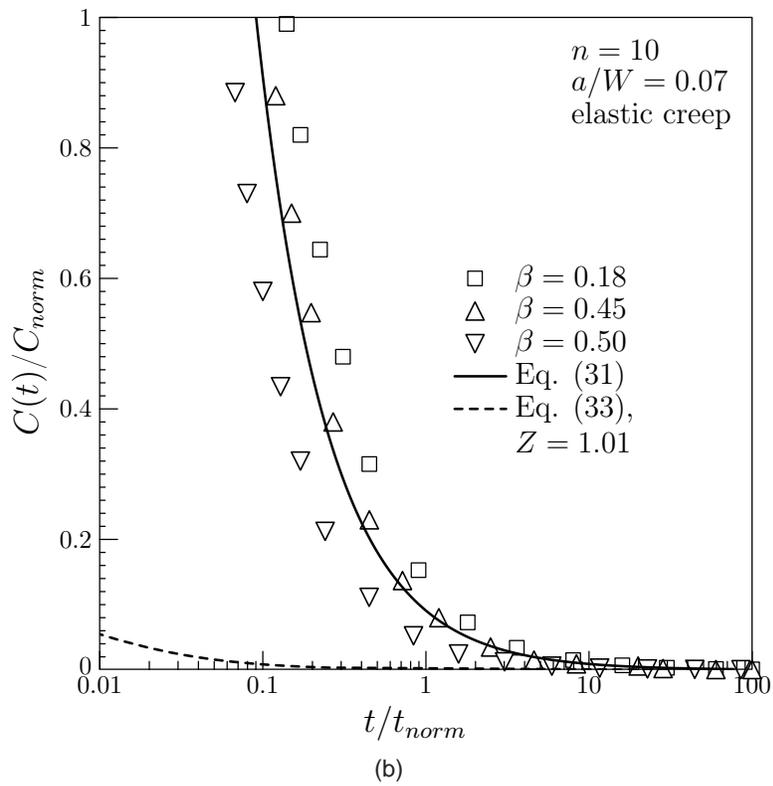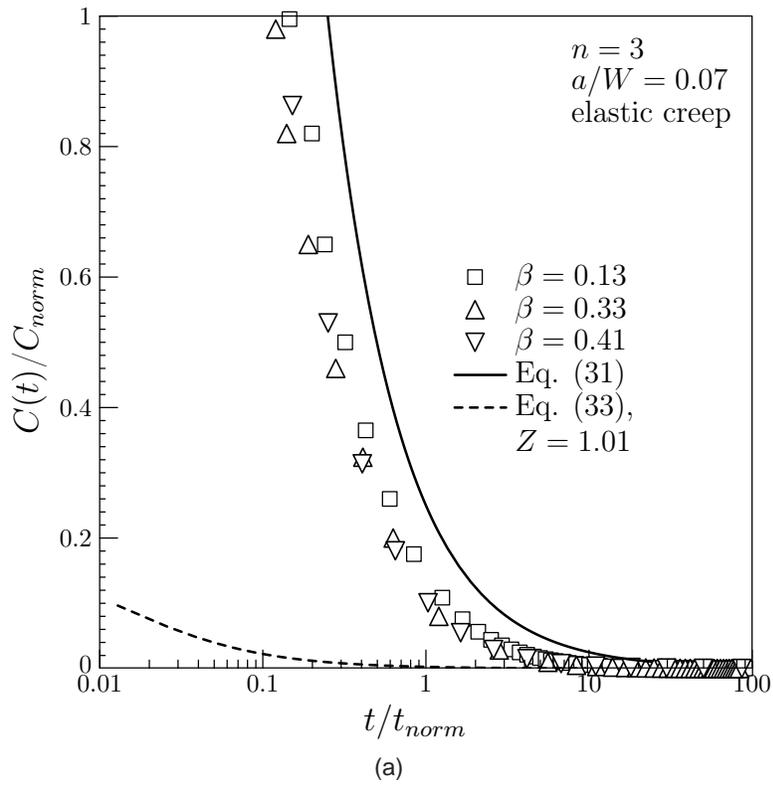
Figure 8: Comparison of evolution of $C(t)$ for elastic-creep conditions under residual stress only at different β values for $a/W = 0.07$; (a) $n = 3$, (b) $n = 10$
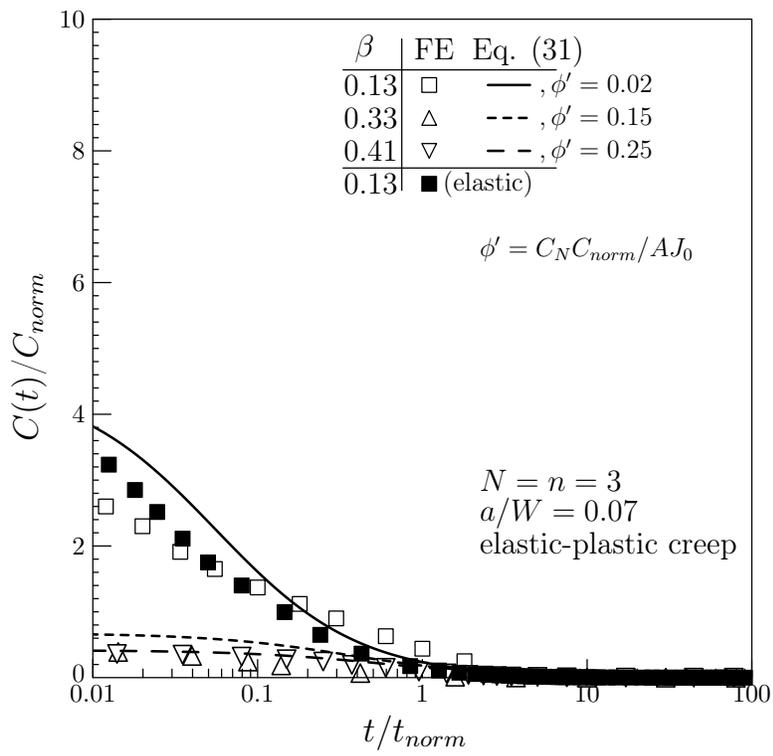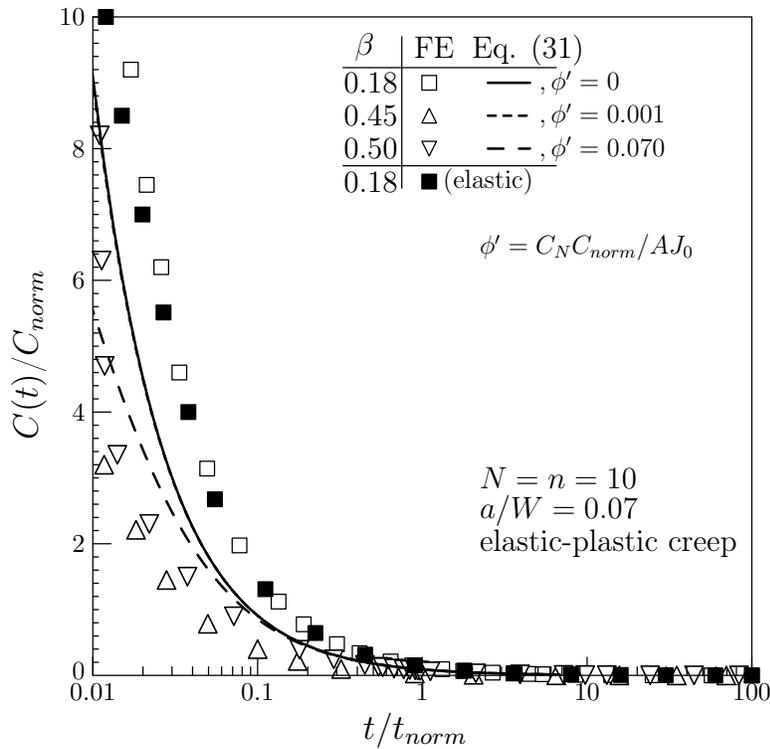
Figure 9: Comparison of evolution of $C(t)$ under elastic-plastic creep conditions under residual stress only at different β values for $a/W = 0.07$; (a) $n = 3$, (b) $n = 10$; elastic-creep results are also included in each case.